JPRS-CST-87-039 035123
2 NOVEMBER 1987

FOREIGN BROADCAST INFORMATION SERVICE

JPRS Report

Science & Technology

China

JPRS-CST-87-039

2 NOVEMBER 1987

SCIENCE & TECHNOLOGY

CHINA

CONTENTS

LIFE SCIENCES

/9986

LIFETIME STUDY OF TRANSVERSE FLOW EXCIMER LASER

40090081 Shanghai GUANGXUE XUEBAO [ACTA OPTICA SINICA] in Chinese Vol 7 No 6, Jun 87 pp 481-485

[English abstract of article by Lou Qihong [2869 4388 3163], et al., of the Shanghai Institute of Optics and Fine Mechanics, Chinese Academy of Sciences]

[Text] The effects of the gas mixture ratio, gas passivation, optical window deposition and laser gas storage time on the lifetime of a transverse flow XeCl excimer laser have been studied in detail. By optimizing these parameters, a lifetime of more than 10^5 pulses was obtained, with a storage time of 1000 hours for one gas fill.

9717

STATIONARY BEHAVIOR OF SINGLE-MODE STANDING-WAVE LASER WITH SATURABLE ABSORBER

40090081 Shanghai GUANGXUE XUEBAO [ACTA OPTICA SINICA] in Chinese Vol 7 No 6, Jun 87 pp 486-492

[English abstract of article by Li Yinggang [2621 2019 0474], et al., of the Physics Department, Northwestern University, Xi'an]

[Text] The Hamiltonian and equation of motion for the order parameter of a single-mode standing-wave laser system with saturable absorber are given in detail. Three stationary solutions of the equation are obtained near the threshold, and their stability is analyzed. The results show that the stationary behavior (nonequilibrium phase transition, bistability, critical exponents) of the standing wave system near the threshold is similar to that of a traveling wave system qualitatively, but differs quantitatively. It is noteworthy that it is possible to realize the I_- (one of the three stationary solutions) branch experimentally, which is not possible in the traveling-wave case.

9717

CuCl LASER-PUMPED WAVEGUIDE DYE AMPLIFIER

40090081 Shanghai GUANGXUE XUEBAO [ACTA OPTICA SINICA] in Chinese Vol 7 No 6, Jun 87 pp 493-500

[English abstract of article by Tang Jinrong [3282 6855 2837], et al., of Shanghai Institute of Optics and Fine Mechanics, Chinese Academy of Sciences]

[Text] Theoretical and experimental studies on a waveguide dye spontaneous emission amplifier are reported. The waveguide mode, ASE threshold and near- and far-field distributions are calculated for a rectangular waveguide model. The output characteristics of the ASE amplifier are studied experimentally. The ASE far-field patterns for the lowest waveguide mode are obtained in agreement with theory.

9717

CYLINDRICAL LENS TEST USING HOLOGRAPHIC INTERFERENCE METHOD

40090081 Shanghai GUANGXUE XUEBAO [ACTA OPTICA SINICA] in Chinese Vol 7 No 6, Jun 87 pp 511-514

[English abstract of article by Zhou Wanzhi [0719 8001 3112], et al., of Changchun Institute of Optics and Fine Mechanics, Chinese Academy of Sciences]

[Text] Cylindrical lenses have been widely used in modern optics, but a satisfactory technique for testing them has not yet been devised. The methods presently available all have some drawbacks.

In this paper, the authors present a new method for testing a cylindrical lens using holographic interferometry. The principle of the method is discussed and the experimental results are given. Also discussed is a method for adjusting the relative position between the slit and cylindrical lens.

This method has several advantages, including simple structure, easy operation and a decrease in the requirements for optical elements. Therefore, this method can be used for routine testing of cylindrical lenses.

9717

MEASUREMENT OF MODE FIELD RADIUS USING EQUIVALENT VARIABLE APERTURE METHOD IN FAR-FIELD OF SINGLE MODE FIBERS

40090081 Shanghai GUANGXUE XUEBAO [ACTA OPTICA SINICA] in Chinese Vol 7 No 6, Jun 87 pp 530-533

[English abstract of article by Bai Aimin [4101 1947 3046] of Wuhan Research Institute of Post and Telecommunications]

[Text] An equivalent variable aperture method for mode field radius measurement of single mode fibers is proposed. It involves measurement of the integrated far-field distribution with a circular aperture moved axially in the far-field of the fiber. In addition, the calculation method for the mode field radius, which is also suitable for non-Gaussian field distributions, is derived using Petermann's new definition of the mode field radius. Experiments show that this method is simple and reliable. The typical deviation of repeated measurements of the mode field radius of a given fiber with different ends is less than 0.04 μm.

9717

INVESTIGATION OF DIGITAL FIBER-OPTIC SYSTEMS WITH BIPHASE CODING AND OPTIMUM TIME DETECTION

40090004 Beijing TONGXIN XUEBAO [JOURNAL OF CHINA INSTITUTE OF COMMUNICATIONS] in Chinese Vol 8 No 2, Mar 87 pp 10-21

[English abstract of article by Lin Rujian [2651 1172 0313] of Shanghai University of Science and Technology]

[Text] This paper deals with the theoretical aspects of an investigation of a biphase coding and time detection scheme for digital fiber-optic communications. It is pointed out that the biphase code is optimal in various line codes for an intensity-modulated digital fiber-optic communications system, whereas the threshold-crossing detection belongs to the statistical test process with a maximum a posteriori probability criterion. Therefore, both can be combined to form an optimum receiver in the sense of a statistical detection theory. Although the conventional amplitude detection detection in a digital fiber-optic communications system does nothing to filter the signal-dependent shot noise of the photon-electron inversion process, the threshold-crossing detection can reduce the effects of all kinds of noise, including the shot noise, to the decision error probability of the system. The research method noted in the references is exploited and extended to the case in which the shot noise should be considered, giving a complete algorithm of shot noise variance, signal-to-noise ratio and error probability for a time detection receiver. The optimization procedure of the receiver filter with the criterion of the maximum signal-to-noise ratio is descrived as well. The results of analysis and computation show that 2-3 dB improvement in receiver sensitivity over the conventional amplitude detection system can be achieved by the biphase coding and threshold-crossing detection system under similar operational conditions.

9717

MEASUREMENT OF OPTIMUM POSITION OF MICROWAVE ANTENNA FEED

40090004 Beijing TONGXIN XUEBAO [JOURNAL OF CHINA INSTITUTE OF COMMUNICATIONS] in Chinese Vol 8 No 2, Mar 87 pp 29-32

[English abstract of article by Yuan Huiren [5913 1920 0088] of Nanjing University]

[Text] The basic method involving using radio sources and satellites as calibration beacons and the Dicke radiometer in the measurement of the optimum position of a microwave antenna feed is presented in this paper. The results show that the measurement of the optimum position of the microwave antenna feed using the method is quite valid. The method can be compared with the geometric optical method--not only does it improve the properties of the antenna sidelobes, but is also increases antenna gain. The method is of considerable practical value.

9717

ANALYSIS AND CALCULATION OF PERFORMANCE OF CONCATENATED CODES OF ELLIOTT COMPOUND CHANNELS

40090004 Beijing TONGXIN XUEBAO [JOURNAL OF CHINA INSTITUTE OF COMMUNICATIONS] in Chinese Vol 8 No 2, Mar 87 pp 64-70, 28

[English abstract of article by Ju Hongqi [7263 1347 3825], et al., of Nanjing Aeronautical Institute]

[Text] In this paper, the authors present and prove the calculating methods and equations for the performance of concatenated codes, with block codes as inner codes and Reed-Solomon codes as outer codes, on Elliott compound channels. They also calculate and analyze the performance of concatenated codes on compound channels, demonstrating that concatenated codes are very good random-and-burst error correcting codes. The authors compare their calculated results with those provided by computer simulation, verifying the effectiveness of the calculating methods developed in this paper.

9717

ENCODING AND DECODING ALGORITHM FOR NONSYSTEMATIC REED-SOLOMON (RS) CODES

40090004 Beijing TONGXIN XUEBAO [JOURNAL OF CHINA INSTITUTE OF COMMUNICATIONS] in Chinese Vol 8 No 2, Mar 87 pp 78-82, 32

[English abstract of article by Zou Shikai [6760 0013 7030] of Beijing Institute of Aeronautics]

[Text] The encoding and decoding algorithm for nonsystematic Reed-Solomon codes is developed in this paper. This is an active algorithm that is based on the Berlekamp and Peterson algorithms and the theorem which calculates the Mattson-Solomon (MS) polynomial from a given polynomial. Its features are that the concept is clear and the sense of the formulae is tangible in addition to its application being convenient. The encoding and decoding algorithm for shortened RS codes is also given.

9717

CALCULATION OF FAR SIDELOBES OF SHAPED CASSEGRAIN ANTENNA USING UTD

40090004 Beijing TONGXIN XUEBAO [JOURNAL OF CHINA INSTITUTE OF COMMUNICATIONS] in Chinese Vol 8 No 2, Mar 87 pp 83-91, 48

[English abstract of article by Nie Zaiping [5119 0961 1627], et al., of Chengdu Institute of Radio Engineering]

[Text] The far sidelobes of shaped Cassegrain antennas with diameters of 11.5 m (for 4 GHz and 6 GHz), 6.2 m (for 4 GHz) and 3 M (for 12 GHz) have been calculated respectively using the uniform geometrical theory of diffraction (UTD). In addition, the measured radiation pattern of the antenna with a diameter of 6.2 m (for 4 GHz) is compared with the corresponding calculated results. Some typical methods for numerical calculation of the transition function in UTD are compared and evaluated in respect to calculation time, accuracy, error distribution and availability to provide some bases for selecting the best calculation method for the given requirements. A new and simple method for calculating the transition function with satisfactory accuracy is introduced in this paper. It has been demonstrated that several relative rays can be merged into one. This ray-merging method has been used in the analysis and calculating of the shaped Cassegrain antennas. Therefore, the calculations are greatly simplified.

9717

CRYSTALLINE QUALITY IMPROVEMENT OF SOS FILMS BY SELF-IMPLANTATION

40090007 Beijing BANDAOTI XUEBAO [CHINESE JOURNAL OF SEMICONDUCTORS] in Chinese Vol 8 No 4, Jul 87 pp 337-344

[English abstract of article by Fan Renyong [5400 0088 3057], et al., of the Institute of Semiconductors, Chinese Academy of Sciences]

[Text] Chemically-deposited silicon vapor on sapphire (SOS) epitaxial films, 0.3-0.54 μm thick, has been implanted with Si ions and recrystallized in the solid phase through furnace annealing and rapid infrared annealing. The improvement in the crystalline quality has been analyzed by MeV He^+ channeling and cross-section transmission electron microscopy. The silicon-sapphire interface width has been measured by Auger electron spectroscopy in combination with Ar^+ sputtering. It is found that the crystalline quality of the epitaxial layer, especially near the interface, can be improved by furnace annealing and rapid infrared annealing. The defect density in the improved layer is much lower than in the as-grown layer. The interface width increased slightly after infrared annealing, but strongly after furnace annealing.

9717

ENERGY BAND STRUCTURE OF METASTABLE SEMICONDUCTOR $(GaAs)_{1-x}(Ge_2)_x$

40090007 Beijing BANDAOTI XUEBAO [CHINESE JOURNAL OF SEMICONDUCTORS] in Chinese Vol 8 No 4, Jul 87 pp 356-361

[English abstract of article by Xu Zhizhong [1776 5267 0022] of the Institute of Modern Physics, Fudan University]

[Text] Using the order parameter S calculated with computer simulation in the (100) planar growth condition of Kim and Stern, the direct energy gap of the metastable semiconductor $(GaAs)_{1-x}(Ge_2)_x$ as a function of composition x has been calculated in the expanded virtual-crystal approximation with the empirical tight-binding method. In the calculation it is thought that the metastable semiconductor alloy keeps the short-range order in any composition x. The results are discussed and compared with experimental findings and preceding theoretical models.

9717

THREE-DIMENSIONAL NUMERICAL SIMULATION OF MOS DEVICES

40090007 Beijing BANDAOTI XUEBAO [CHINESE JOURNAL OF SEMICONDUCTORS] in Chinese Vol 8 No 4, Jul 87 pp 371-377

[English abstract of article by Chen Datong [7115 1129 0681], et al., of the Institute of Microelectronics and Computer Department, Qinghua University]

[Text] Based on the finite difference solution of the respective equations, a computer analysis program, TDMOS-1, for two- and three-dimensional simulation of the characterization of MOS devices has been developed. A self-consistent solution of Poisson's equation and the current continuity equation using Gummel's approach is carried out. The Newton-Raphson algorithm for linearization of the discreted Poisson's equation and the ECCG method for solving linear equations are utilized. By reasonably controlling the Newton iteration times, choosing the appropriate incomplete Cholesky decomposition matrix and taking the two-dimensional analysis results as the initial values for three-dimensional analysis, the computation time is reduced considerably. On a VAXII/750 mainframe, for each potential point, about 20 seconds for two-dimensional analysis and 5 minutes for three-dimensional analysis are needed.

9717

ACCURATE THEORY OF ELECTRICAL AND OPTICAL WAVEGUIDING PROCESSES IN STRIPE-GEOMETRY SEMICONDUCTOR LASER

40090007 Beijing BANDAOTI XUEBAO [CHINESE JOURNAL OF SEMICONDUCTORS] in Chinese Vol 8 No 4, Jul 87 pp 402-409

[English abstract of article by Guo Changzhi [6753 7022 1807], et al., of the Department of Physics, Beijing University]

[Text] The electrical and optical waveguide processes and their interaction in the stripe-geometry semiconductor laser have been treated by an accurate model and detailed, self-consistent computer results have been obtained. It is shown that the usual p-n injection current-voltage relationship and any imposed-fixed shape injection current distribution should not be used as bases for analyzing waveguide behavior in the stripe-geometry semiconductor laser. The so-called self-focusing mechanism of the kink in the optical power-current characteristics has also been examined.

9717

CRITERIA FOR EVALUATING COGENERATION AND BASIC ANALYSIS OF GAS TURBINE COGENERATION

40090009 Beijing GONGCHENG REWULI XUEBAO [JOURNAL OF ENGINEERING THERMOPHYSICS] in Chinese Vol 8 No 3, Aug 87 pp 201-205

[English abstract of article by Cai Ruixian [5591 4213 6343] of the Institute of Engineering Thermophysics, Chinese Academy of Sciences]

[Text] In order to evaluate the cogeneration more exactly, in addition to the total energy efficiency and exergy efficiency in common use, another criterion is proposed to evaluate the performance of cogeneration. This criterion is defined as obtaining maximum total income by selling power and heat with a given fuel consumption. Using these criteria, the optimum values of gas turbine cogeneration design parameters and the relative influences of some parameters are derived analytically under some general simplified conditions.

9717

IMPROVEMENT OF AERODYNAMIC CALCULATION ON S_{2m} STREAM SURFACE OF AXIAL COMPRESSOR USING ANNULUS WALL BOUNDARY LAYER CALCULATION

40090009 Beijing GONGCHENG REWULI XUEBAO [JOURNAL OF ENGINEERING THERMOPHYSICS] in Chinese Vol 8 No 3, Aug 87 pp 230-236

[English abstract of article by Wang Qinghuan [3076 1987 2719], et al., of the Institute of Engineering Thermophysics, Chinese Academy of Sciences]

[Text] This paper presents an approach toward improving the aerodynamic calculations on S_{2m} (S stream surface) by employing the annulus wall boundary layer (AWBL) calculation technique. A simplified formula for transforming the displacement thickness of AWBL into the mass flow blockage coefficient conventionally used in S_{2m} calculations is proposed. The inviscid-viscid iterative calculations using three different schemes have been carried out to investigate the blockage effects of AWBL on the S_{2m} calculation. The results of improved S_{2m} calculations for both a single-stage and a 10-stage axial compressor are compared with those measured by a Laser-Two-Focus velocimeter in a compressor rotor.

9717

SOLUTION FOR TRANSONIC FULL-POTENTIAL BLADE-TO-BLADE FLOW BY MULTIGRID METHOD

40090009 Beijing GONGCHENG REWULI XUEBAO [JOURNAL OF ENGINEERING THERMOPHYSICS] in Chinese Vol 8 No 3, Aug 87 pp 237-242

[English abstract of article by Ji Wei [1323 4850], et al., of the Institute of Engineering Thermophysics, Chinese Academy of Sciences]

[Text] Based on the principle of the multigrid method, a very effective solution method for transonic full-potential blade-to-blade flow in turbomachinery is presented. The computational results are compared with the experimental data and with other numerical calculations. When comparing this multigrid method with the traditional single grid method, the computational results show that about 60 percent of the CPU time can be saved under the same grid spacing and with the same convergence accuracy, or the convergence accuracy can be improved by 2 orders for multigrid calculation if the CPU consumption for both calculations is the same. A reasonable treatment for the leading edge is also presented based on the conservation performance of the full-potential equation.

9717

LAMINAR FILM CONDENSATION OF FREON IN PRESENCE OF AIR OF NONHOMOGENEOUS CONCENTRATION

40090009 Beijing GONGCHENG REWULI XUEBAO [JOURNAL OF ENGINEERING THERMOPHYSICS] in Chinese Vol 8 No 3, Aug 87 pp 249-254

[English abstract of article by Wei Baotai [7614 0202 1132], et al., of Tianjin University]

[Text] An analytical model is presented for the laminar film condensation of freon in the presence of air of nonhomogeneous concentration, and the boundary layer equations are solved using the integration technique. The profiles of the gas-vapor boundary layer thickness, condensate film thickness, interface temperature and local heat transfer flux are calculated, and the mode of the effect of nonhomogeneity of noncondensable gas on heat transfer that was neglected in the previous studies is revealed in the calculation.

Also presented in this paper is experimental research on the R_{113}-Air mixture along a vertical surface. The agreement between the theoretical and experimental results is satisfactory.

9717

STUDIES OF LOCAL HEAT TRANSFER AROUND HORIZONTAL TUBE IN LARGE PARTICLE FLUIDIZED BED

40090009 Beijing GONGCHENG REWULI XUEBAO [JOURNAL OF ENGINEERING THERMOPHYSICS] in Chinese Vol 8 No 3, Aug 87 pp 255-259

[English abstract of article by Hu Jia [5170 0163], et al., of the Institute of Engineering Thermophysics, Chinese Academy of Sciences]

[Text] This paper describes an experimental investigation of the local heat transfer around a horizontal tube in a large particle fluidized bed. It is shown that the distribution of local heat transfer coefficients for a tube in a large particle fluidized bed is quite different from that in a small praticle fluidized bed. The local heat transfer for the tube at the 0° point of the upwind is about 20-40 percent higher than that at the 180° point of the downwind. The distributions of the heat transfer coefficients are discussed from the point of view of bubble dynamics.

9717

ATMOSPHERIC PARTICULATES AND ACID RAIN

Beijing ZHONGGUO HUANJING KEXUE [CHINA ENVIRONMENTAL SCIENCE] in Chinese Vol 7 No 2, Apr 87 pp 1-8

[English abstract of article by Zhao Dianwu [6392 3013 0063], et al., of the Institute of Environmental Chemistry, Chinese Academy of Sciences, Beijing; Xiong Jiling [3574 7139 5044], et al., of Guizhou Institute of Environmental Science, Guiyang]

[Text] Samples of total suspended particulates and particles in different size ranges were collected at urban and rural areas in Guiyang, Chongqing and Beijing. Experiments involving the relationship of the buffering capacity of airborne particulates to acidification were conducted using these samples.

Particulates in Guiyang and Chongqing had higher acidity and much lower buffering capacity when compared to those in Beijing. Along with decreasing in size, the acidity of particles increased while the buffering capacity decreased. This was due to the fact that the SO_4^{2-} content was higher and the Ca^{2+} content lower in fine particles than in coarse particles. Experiments involving the buffering capacity of airborne particles and below-cloud scavenging of SO_2 in air showed that atmospheric particulates were able to neutralize almost half of the acid in precipitation. The washout of particulates is the major source of SO_4^{2-}, Ca^{2+} and NH_4^+ in precipitation.

9717
CSO: 4009/3034

BELOW-CLOUD SCAVENGING OF SO AND ORIGIN OF ACID IN PRECIPITATION IN GUIYANG

Beijing ZHONGGUO HUANJING KEXUE [CHINA ENVIRONMENTAL SCIENCE] in Chinese Vol 7 No 3, Jun 87 pp 36-42

[English abstract of article by Xiong Jiling [3574 7139 5044], et al., of Guizhou Institute of Environmental Science, Guiyang; Zhao Dianwu [6392 3013 0063] of the Institute of Environmental Chemistry, Chinese Academy of Sciences, Beijing]

[Text] Experiments conducted at three sites of different types in Guiyang showed that below-cloud scavenging of SO_2 in air is an overwhelming source of acid in precipitation, and nearly half of it is subsequently neutralized by airborne particles and gaseous ammonia. Concentrations of S(IV), H^+ and SO_4^{2-} in precipitation have a temporal and spatial distribution similar to that of SO_2 in air, i.e., high in urban areas and cold seasons and low in rural areas and warm seasons. Below-cloud scavenging of SO_2 contributes less than 30 percent of the total precipitation sulfur, with the rest mainly coming from the washout of atmospheric particulates. A mathematical model established based on the experimental results of SO_2 washout can give precipitation acidity and chemical composition quite close to those actually measured.

9717
CSO: 4009/0034

RESEARCH ON GASOLINE ADDITIVES WHICH CAN REDUCE POLLUTION OF EXHAUST GAS

Beijing ZHONGGUO HUANJING KEXUE [CHINA ENVIRONMENTAL SCIENCE] in Chinese Vol 7 No 3, Jun 87 pp 55-58

[English abstract of article by Hu Jiajun [5170 1367 0193] of Beijing Polytechnic University; Zhang Fan [1728 0416] of the Chinese Research Academy of Environmental Sciences, Beijing]

[Text] In order to reduce exhaust gas pollution and raise the combustion heat of gasoline (70#), the authors used the oxygen bomb method for evaluating 14 additives, including iron, manganese, zinc, cobalt, nickel and copper chelates of β-diacetone. These additives can reduce total hydrocarbons and nitric oxides in the exhaust gas as well as raise the combustion heat of the gasoline. The best results were obtained from the manganese, zinc and cobalt chelates of β-dibenzoyl ferrocene.

9717
CSO: 4009/3034

MOLECULAR EVOLUTION OF POLIO VIRUSES

Beijing YICHUAN XUEBAO [ACTA GENETICA SINICA] in Chinese Vol 14 No 3, Jun 87 pp 206-210

[English abstract of article by Yang Xiaofeng [2799 2556 1496], et al., of the Insittute of Medical Biology, Chinese Academy of Medical Sciences, WHO Collaborating Center for Reference and Research on Enteroviruses, Kunming]

[Text] According to the data of the genomic nucleotide sequences and the amino acid sequences of the viral proteins of reference strains in all three types of polio viruses, the first attempt was made to calculate intertypic evolutionary distance, intertypic divergence time and the rates of amino acid substitution of polio virus proteins between the strains using the calculating method based on Kimura's molecular evolution theory. The results showed: (1) the evolutionary distances between types in all three types of polio viruses were almost equal; (2) three types of polio viruses were almost simultaneously evolved from a common ancestor virus 1000-2000 years ago; (3) the rates per site per year of the amino acid substitutions among the three polio virus types were also similar.

9717
CSO: 4009/3031

ULTRASTRUCTURAL STUDY OF PIECEMEAL NECROSIS IN CHRONIC ACTIVE HEPATITIS

40093041 Beijing ZHONGHUA BINGLIXUE ZAZHI [CHINESE JOURNAL OF PATHOLOGY] in Chinese Vol 16 No 2, 30 Jun 87 pp 83-85

[English abstract of article by Zhang Taihe [1728 1132 0735] of Nanjing Command General Hospital, PLA]

[Text] Piecemeal necrosis (PN) is one of the most important histologic diagnostic criteria in chronic active hepatitis (CAH). In order to evaluate the relationship between the hepatocytic necrosis and inflammatory responses, liver biopsies from 250 cases of CAH were investigated under light and electron microscopes. The results suggest that lymphocytes are the major component of the infiltrating mononuclear cells presented in PN areas and are in close contact with hepatocytes, simultaneously producing parenchymatous apoptosis. These lymphocytes are believed to play an important role in the perpetuation of liver damage. In milder forms of CAH, plasma cells are scanty in these areas. When the PN lesions expanded into BN (bridging necrosis), plasma cells often increased in number. Therefore, the antibody producing plasma cells may be another important factor in inducing hepatocytolysis in moderate or severe forms of CAH.

9717

PRELIMINARY INVESTIGATION OF RELATIONSHIP BETWEEN EXPRESSION OF HBV ANTIGENS AND LIVER CELL NECROSIS

40093041 Beijing ZHONGHUA BINGLIXUE ZAZHI [CHINESE JOURNAL OF PATHOLOGY] in Chinese Vol 16 No 2, 30 Jun 87 pp 86-89

[English abstract of article by Hu Keqin [5170 0344 0530], et al., of Tongji College of Medical Sciences]

[Text] The relationship between expressive patterns of hepatitis B surface antigen (HBsAg) and core antigen (HBcAg) and liver cell necrosis of 90 patients with chronic liver disease has been analyzed. The results suggest that the membranous expression of HBsAg and HBcAg is associated with the activity of liver disease. Cytoplasmic-membranous HBcAg may be the main target antigen attacked by host immune systems to cause liver cell necrosis, but the possibility of a relationship between the membranous expression of HBsAg and liver cell necrosis has not been ruled out. In this article, factors affecting the host immune function and the relationship between the membranous expression of HB Ag and liver cell necrosis are discussed.

9717

IMMUNOHISTOCHEMICAL STUDY OF HBcAg IN LIVER OF PATIENTS WITH TYPE B HEPATITIS

40093041 Beijing ZHONGHUA BINGLIXUE ZAZHI [CHINESE JOURNAL OF PATHOLOGY] in Chinese Vol 16 No 2, 30 Jun 87 pp 90-93

[English abstract of article by Tan Chengxiang [6223 2110 7309], et al., of Beijing College of Medical Sciences]

[Text] In order to detect the presence of HBcAg, the ABC staining technique was applied to formalin-fixed paraffin liver sections from 153 post-morten liver specimens collected during the past 32 years. The expression patterns of HBcAg in liver cells are divided into two types: nuclear HBcAg (N-HBcAg) and cytoplasmic membranous HBcAg (CM-HBcAg). The CM-HBcAg was expressed clearly in liver cells using this method. The morphological appearance of CM-HBcAg is described in detail.

Results indicate that there is a close relationship between the expression of CM-HBcAg and liver necrosis. HBcAg distributed on the liver cell membrane may be one of the important target antigens. N-HBcAg, on the other hand, might be associated only with the expressive pattern found in some healthy HBcAg carriers rather than with liver injury.

9717

FAT STORING CELLS (FSC) AND HEPATIC FIBROGENESIS--TRANSFORMATION OF FSC IN CHRONIC VIRAL HEPATITIS

40093041 Beijing ZHONGHUA BINGLIXUE ZAZHI [CHINESE JOURNAL OF PATHOLOGY] in Chinese Vol 16 No 2, 30 Jun 87 pp 97-99

[English abstract of article by Xi Yuping [1598 5280 1627], et al., of Beijing College of Medical Sciences]

[Text] Eight liver biopsies from patients suffering from chronic active hepatitis (CAH) and chronic persistent hepatitis (CPH) were collected. Observation of the ultrastructural changes in the fat storing cells (FSC) and a comparison of the volume densities of lipid droplets in FSC were done with Videoplan MOP 40. The percentages of transitional cells in these two types of hepatitis were also analyzed. Lipid droplets in the majority of FSC in CAH decreased both in number and volume, while the endoplasmic reticula increased and dilated. The volume density of lipid droplets in FSC was an average of 0.150 ± 0.072 in CAH, but 0.33 ± 0.082 in CPH, with $P < 0.001$. The percentage of transitional cells was 78 percent in the former and 18 percent in the latter. Results clearly show that FSC are capable of transforming into fibroblasts in chronic viral hepatitis based on the morphological description and changes in the volume density of the lipid droplets as well as the higher percentage of transitional cells present in CAH. Therefore, transformation of FSC is a critical step in the pathogenesis of hepatic fibrogenesis from CAH.

9717

EXPERIMENTAL INFECTION OF HUMAN HEPATITIS B VIRUS (HBV) IN ADULT TREE SHREWS

40093041 Beijing ZHONGHUA BINGLIXUE ZAZHI [CHINESE JOURNAL OF PATHOLOGY] in Chinese Vol 16 No 2, 30 Jun 87 pp 103-106

[English abstract of article by Su Jianjia [5685 1696 1367], et al., of Guangxi Zhuang Autonomous Region Tumor Research Institute]

[Text] Ninety-six tree shrews were inoculated with 0.5 ml human serum containing HBV through the femoral vein and in the abdominal cavity. Four tree shrews inoculated with bovine serum and five others with no serum administration were used as the controls. Before inoculation, all 105 animals tested negative for HBsAg and anti-HBs in sera known beforehand. After inoculation, 79 of the group of 96 tree shrews tested positive for HBsAg and/or anti-HBs through PHA, and 49 tested positive for HBV DNA by the molecular hybridization test. In addition, 22-nm spherical and tubular form HBsAg particles and a small amount of 42-nm Dane particles were observed in the sera samples of three animals. In liver biopsies from nine sera-HBsAg positive animals, eight tested positive for HBsAg in the cytoplasm and two for HBcAg in the nucleus. No positive results were obtained in the nine controls.

Liver specimens showed spotty necrosis and portal inflammation among the infected animals by light microscopy, and a few liver cells showed ballooning degeneration.

Results suggest that the tree shrew is susceptible to human HBV inoculation. The incidence can reach 90.6 percent, and the HBs antigenemia can persist for up to 16 weeks.

9717

STUDY OF MORPHOMETRY OF GIANT PLATELETS IN PERIPHERAL BLOOD OF PATIENTS WITH EPIDEMIC HEMORRHAGIC FEVER

40093041 Beijing ZHONGHUA BINGLIXUE ZAZHI [CHINESE JOURNAL OF PATHOLOGY] in Chinese Vol 16 No 2, 30 Jun 87 pp 144-146

[English abstract of article by Guo Ning [6753 1337], et al., of the PLA College of Military Medical Sciences]

[Text] A Quantimet 920 automatic image analyzing instrument was used for the quantitative analysis of giant platelets of patients with epidemic hemorrhagic fever. Morphologic changes in the platelets included loss of the discoid shape, frequent extrusion of pseudopods, a variation in the platelet size, an increased volume of many platelets and frequent occurrence of giant and abnormal platelets. Results of the image analysis indicate that the average size (area) of the platelet (6.69 μm^2) of patients is remarkably larger than that of those of normal persons (3.49 μm^2), with $P < 0.001$. The occurrence of giant platelets (90 percent) is considered favorable for making an early diagnosis.

9717

ANTI-INFLAMMATORY AND ANALGESIC ACTIONS OF YUNACONITINE

40093040 Beijing ZHONGGUO YAOLIXUE YU DULIXUE ZAZHI [CHINESE JOURNAL OF PHARMACOLOGY AND TOXICOLOGY] in Chinese Vol 1 No 2, Feb 87 pp 93-99

[English abstract of article by Lin Zhigong [2651 1807 1562], et al., of Shanghai Institute of Materia Medica, Chinese Academy of Sciences]

[Text] Yunaconitine (YAc) has been extracted from several plants of Aconitum in China since 1955, but its pharmacological action has not yet been investigated in detail. In this paper, the anti-inflammatory and analgesic actions of YAc are reported. When given subcutaneously (10-80 μg/kg) or orally (50-100 μg/kg) in rats and mice, YAc inhibited the increased vascular permeability caused by acetic acid and histamine, the leucocyte migratory response induced by the injection of 1 percent carrageenin 0.1 ml in a rat's thoracic cavity, and the swelling of a mouse ear caused by xylene and edema of the hind paw elicited by carrageenin, fresh egg whites or formaldehyde in intact or adrenalectomized rats. YAc also showed positive effects in the granuloma inhibition test when it was subcutaneously injected, 10 μg/kg for 6 d, or added directly to the cotton pellet. The fact that YAc neither reduced the weights of the thymus and adrenal in the rats nor prolonged the survival time in adrenalectomized rats indicates that the action of YAc does not depend on stimulation of the pituitary-adrenal axis.

Assayed with the writing and hot plate method, the median analgesic doses (ED_{50}) of YAc were found to be 39 and 42 μg/kg in mice, respectively. YAc was shown to have an antithermic effect in pyrexial rats when administered orally at a dosage of 50 μg/kg.

9717

IMMUNOMODULATING ACTIONS OF YUNACONITINE

40093040 Beijing ZHONGGUO YAOLIXUE YU DULIXUE ZAZHI [CHINESE JOURNAL OF PHARMACOLOGY AND TOXICOLOGY] in Chinese Vol 1 No 2, Feb 87 pp 100-104

[English abstract of article by Li Xiaoyu [2621 2556 3768], et al., of the Shanghai Institute of Materia Medica, Chinese Academy of Sciences]

[Text] Yunaconitine (YAc) is an alkaloid isolated from Aconitum hemsleyanum Pritz. var. circinatum W.T. Tang and Aconitum geniculatum Flet. et Laue. var. unguiculatum W.T. Wang. It is not only highly toxic, but also highly active biologically. Recently, anti-inflammatory, analgesic and antipyretic effects were found at very low dosages. In this paper, immunomodulating actions of YAc are reported.

Split heart tissues of newborn C57/BL mice were transplanted into adult male ICR mice ear pinna. The ECGs were followed every day to judge the survival time of the allografts. YAc 50 μg/(kg·d) ip from the second day after heart transplantation markedly prolonged the survival time of the allografts and was comparable to the well-known immunosuppressor prednisolone. When given from the seventh day after the operation, no marked effect of either drug was observed. A tendency toward inhibited delayed type of hypersensitivity to the EAE antigen was observed in EAE rats administered with YAc 5 and 10 μg/kg ip.

YAc ip 20 μg/kg x 4 d showed no definite inhibition on serum hemolysin and IgG levels, while 50 μg/kg x 3 d suppressed the spleen PFC counts of SRBC challenged C57/BL mice. It was noted that YAc increased the serum total complement as well as the phagocytic activity of the reticuloendothelial system in mice. These effects are considered to be beneficial in the clearance of pathogenic antigens, and may be the immunopharmacological basis of anti-inflammatory actions of YAc.

9717

EFFECTS OF NEUROTOXIN IN COBRA VENOM ON CONTENTS OF ENKEPHALINS IN RAT BRAIN AND CONTRACTIONS OF GUINEA PIG ILEUM AND MOUSE VAS DEFERENS

Hebei ZHONGGUO YAOLIXUE YU DULIXUE ZAZHI [CHINESE JOURNAL OF PHARMACOLOGY AND TOXICOLOGY] in Chinese Vol 1 No 3, May 87 pp 166-171

[English abstract of article by Chen Ruzhu [7115 3067 4591], et al., of the Department of Pharmacology, Sun Yat-sen University of Medical Sciences, Guangzhou]

[Text] Changes in the contents of Leu-enkephalin-like and Met-enkephalin-like immunoreactive substances (LEK ir and MEK ir) in rat's brains were studied after the rats were injected with cobrotoxin (NT) for 7 days. The effects of NT on the contractions of the guinea pig ileum and mouse vas deferens induced by electrical stimulation were also investigated in order to explore the analgesic mechanism of NT.

Thirty-five rats were divided into a control group and a NT group. The rats were in normal saline and NT, respectively, for 7 days. The contents of MEK ir and LEK ir in the hypothalamus, striatum, midbrain and thalamus, hippocampus and hindbrain were measured by radioimmunoassay. The results show that the contents of both MEK ir and LEK ir in the hypothalamus and midbrain-thalamus NT group were significantly higher ($p < 0.05$) than those of the control group, while no obvious changes of those contents were noted in the hippocampus and hindbrain NT groups.

Contractions of both the guinea pig ileum and mouse vas deferens were markedly suppressed by morphine in low concentration. Such effects were not interfered with by NT, but could be completely antagonized by naloxone.

These results suggest that NT does not directly interact with morphine receptors, but the analgesic mechanism of NT may be involved with the endogenous opioid peptidergic systems in the central nervous system.

9717
CSO: 4009/3033

ELECTROPHYSIOLOGICAL EFFECTS OF CHINESE COBRA VENOM ON ISOLATED SINOATRIAL NODE AND PAPILLARY MUSCLE OF RAT

Hebei ZHONGGUO YAOLIXUE YU DULIXUE ZAZHI [CHINESE JOURNAL OF PHARMACOLOGY AND TOXICOLOGY] in Chinese Vol 1 No 3, May 87 pp 172-176

[English abstract of article by Wang Yuliang [3769 3768 5328], et al., of the Central Laboratory, Shanxi Institute of Traditional Chinese Medicine, Taiyuan]

[Text] The electrophysiological properties and inotropic effects of Chinese cobra venom on isolated sinoatrial nodes and papillary muscles of rats were observed using a glass microelectrode and an in vitro perfusion technique.

The experimental results show that the Chinese cobra venom (1 μg/ml for 5 min) induced marked negative chronotropic effects, with the sinus cycle length prolonged by 150 ± SD70 ms ($p < 0.05$), the rate of phase 4 depolarization slowly decreased by 57.1 ± SD3.5 mV/s ($p < 0.05$), the maximum diastolic potential declined by -52.0 ± SD3.0 mV and the action potential terminated by "irreversible depolarization."

In particular, the Chinese cobra venom frequently induced the diastolic potential's "oscillatory phenomena," which evoked phase 4 depolarization irregularities with abnormal repolarization, and triggered premature depolarization.

In addition, Chinese cobra venom (1 μg/ml for 3 min) also induced marked negative inotropic effects on papillary muscle preparations. It is suggested that Chinese cobra venom might include a "cardiotoxin-like" fraction.

9717
CSO: 4009/3033

TOXICOKINETICS OF SULFUR MUSTARD

Hebei ZHONGGUO YAOLIXUE YU DULIXUE ZAZHI [CHINESE JOURNAL OF PHARMACOLOGY AND TOXICOLOGY] in Chinese Vol 1 No 3, May 87 pp 188-194

[English abstract of article by Zhang Baozhen [1728 1405 4176], et al., of the Institute of Pharmacology and Toxicology, Academy of Military Medical Sciences, Beijing]

[Text] The toxicokinetics of sulfur mustard (SM) in vivo and in blood and skin homogenates of humans and piglets in vitro have been studied. SM was measured by a sensitive and specific gas chromatographic technique with a flame photometric detector.

The elimination of SM from normal saline, plasma, erythrocyte suspensions of piglet and whole blood, and 2 percent skin homogenates of humans and piglets in vitro were characterized by first-order kinetics. The $t_{\frac{1}{2}}$ of SM in normal saline was 4.80 min, and in other biosamples were 4-7 min.

The time course of SM concentration in piglet blood following iv SM 10 mg/kg fit the three-compartment open model. Following a subcutaneous injection of SM, the toxicokinetics of SM in the piglets appeared to fit a first-order absorption one-compartment open model. No SM was detected in the blood when SM was given percutaneously.

The toxicokinetic characteristics of SM in piglets were as follows: 1. SM could be absorbed rapidly after subcutaneous injection. The half-life of absorption ($t_{\frac{1}{2}}ka$) was 7.45 min; 2. The rate of distribution of SM was very quick. Within 2.5 min following a 10 mg/kg intravenous injection, 90 percent of the SM had been lost from systemic circulation. The time required to reach distribution equilibrium between compartments was less than 7 min; 3. There was a combinative store of SM in the piglets. During the postdistributive phase, the fraction of SM in the central compartment was only 7 percent of the total SM in the entire body. The V_b was 2.47 l/kg, which was three times the total volume of body water; 4. The elimination of SM in the piglet was rapid, with a half-life of 12.0 min.

9717
CSO: 4009/3033

RADIOIMMUNOASSAY FOR T2 TOXIN

Hebei ZHONGGUO YAOLIXUE YU DULIXUE ZAZHI [CHINESE JOURNAL OF PHARMACOLOGY AND TOXICOLOGY] in Chinese Vol 1 No 3, May 87 pp 195-199

[English abstract of article by Rong Kangtai [2837 1660 3141], et al., of the Institute of Pharmacology and Toxicology, Academy of Military Medical Sciences, Beijing]

[Text] A method for RIA of T2 has been developed. A T2-BSA conjugate and [^{3}H]T2 were synthesized as described by Chu, et al., and Wallace, et al., respectively. An anti-T2 antiserum with an average affinity constant of 3.2×10^9 M^{-1} was obtained from immunized rabbits. The assay procedure is described briefly as follows: 5 min after mixing 0.20 ml antiserum (1:1000 dilution) with 0.10 ml sample, 0.10 ml [^{3}H]T2 (0.70 ng) is added to the mixture, which is then incubated at 0°C and pH 8.0 for 1 hour. The bound fraction is separated from the free fraction by adding dextran-coated charcoal and centrifugation. The supernatant is decanted on glass fiber filter papers for scintillation counting. The detection limit of T2 in water is 0.10 ng (1.0 ng/ml), while that of T2 in the blood of rats, rabbits and humans and in human urine is 0.20 ng (2.0 ng/ml). Intra-assay and inter-assay coefficients of variation are lower than 9 percent and 12 percent, respectively. Cross-reactivities of acetyl T2, HT2 and T2-triol are 190 percent, 20 percent and 0.13 percent, respectively. No cross-reactivity was observed with T2-tetraol or verrucarin A.

9717
CSO: 4009/3033

PRODUCTION AND CHARACTERIZATION OF MONOCLONAL ANTIBODIES AGAINST CUCUMBER MOSAIC VIRUS

Beijing WEISHENGWU XUEBAO [ACTA MICROBIOLOGICA SINICA] in Chinese Vol 27 No 2, Jun 87 pp 128-133

[English abstract of article by Gu Dengfeng [6253 4098 1496], et al., of the Veterinary Institute, Xingjing Academy of Husbandry, Urumqi; Kang Liangyi [1660 5328 0308], et al., of the Institute of Microbiology, Chinese Academy of Sciences, Beijing; Chen Jing [7115 0079], et al., of the Institute of Plant Quarantine, Ministry of Agriculture, Animal Husbandry and Fishery, PRC, Beijing]

[Text] Six monoclonal antibodies to CMV were obtained by fusion of SP 2/0 myoloma cells with spleen cells from BALB/C mice immunized with CMV. They belong to the IgM subgroup.

The blocking test, neutralization test and cross-reaction with different viruses showed that the six monoclonal antibodies were specific to CMV and cross-reacted with CMV-Q, CMV-P and CMV-B, but did not with CMV-6 and TAV. They did not cross-react with eight other species of plant viruses used.

9717
CSO: 4009/3032

FERMENTATION, ISOLATION AND PHYSICO-CHEMICAL PROPERTIES OF YOULEMYCIN

Beijing WEISHENGWU XUEBAO [ACTA MICROBIOLOGICA SINICA] in Chinese Vol 27 No 2, Jun 87 pp 156-164

[English abstract of article by Ye Xuwei [0673 4872 1983], et al., of the Institute of Microbiology, Chinese Academy of Sciences, Beijing]

[Text] Streptomyces sp. No C-19 was isolated from soil samples collected on Youle mountain at Xishuangbanna in Yunnan. The strain was found to produce a new antibiotic--Youlemycin--and a minor component.

A high yield of Youlemycin was obtained in a soymeal-glucose medium and isolated by Amberlite IRC-50 resin column from the culture broth. The substance was purified by chromatography on a Nankai D 151 macroreticular resin column and CM-Sephadex C25.

Youlemycin exhibits a broad antibacterial spectra, especially against most of the aminoglycoside-resistant organisms (Staphylococcus aureus, Pseudomonas aeruginosa, etc.). It is a new aminocyclitol antibiotic, which is related to apramycin and saccharocin (antibiotic KA-5685). Youlemycin is a colorless powder having the empirical formula $C_{23}H_{45}N_5O_{12}$ (MW 583 by FAB mass spectra), m.p. 162-165°C (dec) and $[\alpha]_D^{26}$ + 137.8° in water. It has no characteristic absorption maxima in the ultraviolet spectrum. It can form salts with inorganic acids. Based on its unique ultraviolet spectrum, infrared spectrum, nuclear magnetic resonance spectra, FAB mass spectra and compared with kanamycin A or B, apramycin and tobramycin, it is judged to be a novel aminoglucoside type of compound.

9717
CSO: 4009/3032

NEW SUBSPECIES OF MICROMONOSPORA GENUS PRODUCING AMINOGLYCOSIDE ANTIBIOTICS

Beijing WEISHENGWU XUEBAO [ACTA MICROBIOLOGICA SINICA] in Chinese Vol 27 No 2, Jun 87 pp 181-185

[English abstract of article by Zhu Jianping [2612 1017 1456], et al., of Jiangsu Institute of Microbiology, Wuxi]

[Text] The microorganism Micromonospora strain M-41 was obtained from ooze samples in Wuxi, Jiangsu. It was found to produce Sisomicin and Verdamicin. Its morphological cultural characteristics, utilization of various carbon and physiological properties were studied. It is different from any known species. It produced dark green to greenish-black substrate mycelia and greenish-black to black spores. Under an electron microscope, the spore appeared to be oval to spherical in shape, with a bluntly sping-surface. There was no aerial mycelium and no soluble pigment. This strain, M-41, was considered to be a new subspecies of Micromonospora, and therefore the name Micromonospora olivoasterospora subsp. wuxiensis is proposed.

9717
CSO: 4009/3032

TRENDS IN DEVELOPMENT OF CHINESE IRON, STEEL INDUSTRY SURVEYED

Beijing GANGTIE [IRON AND STEEL] in Chinese Vol 22, No 4, Apr 87 pp 1-10

[Article by Shao Xianghua [6730 6272 5478], Central Iron and Steel Research Institute: "Development and Prospects of China's Iron and Steel Industry"]

[Summary] The fluctuations of the world steel industry in the 1970's show that despite economies of scale, large-scale steel production lacks the ability to adapt to changing supply and market conditions. There has always been some advantage to small-scale production, which in the past involved refining of steel scrap in electric furnaces. But many new technologies suited to small-scale production are now being developed in order to increase flexibility and competitiveness, while the older technologies are being improved.

While China was fourth in the world in total steel output in 1983, its 1986 per-capita output was only 50 kg, a third of the world average per capita level. Both assortment and quality are inadequate, and China's import of steel is increasing: it may be the world's largest steel importer in 1987.

In the postwar period, with Soviet help, China expanded the iron and steel works at Anshan and rebuilt those at Wuhan and Baotou and some specialty steel plants, all using the blast furnace-open hearth furnace cycle.

In the 1950's to deal with a steel shortage, a new approach in which cupola-furnace steel was refined with an air blast in small side-blown converters was added. The technology was suited to small facilities with converter capacities of 6 tons or less and led to widespread development of small steel works. Most of these facilities were subsequently converted to top-blown converters using oxygen, often with an increase in capacity to 10-20 tons or more. Larger facilities were also added.

While isolated from the rest of the world, China built the Panzhihua Iron and Steel Complex. A special Chinese-developed process was used in its blast furnace to deal with ore that was high in titanium dioxide. The Baoshan Iron and Steel Complex, built later with imported foreign technology and put into service in 1985, is a copy of a large-scale Japanese steel works.

There are now 10-odd "key" enterprises with annual outputs of from 1 to 7 million tons, most of them integrated iron and steel complexes; they have

capacities from 100,000 to 500,000 tons and primarily refine steel scrap in electric furnaces. There are about 30 local mainstay enterprises with capacities of 5 to 50 tons, mostly developed from the small local facilities of the 1950's. China's main steel works are shown in Fig. 2.

The distribution of blast-furnace size is shown in Fig. 3 and the distribution of converter, open-hearth furnace and electric-furnace capacities in Fig. 4. Many small plants have the potential for increasing their output by improving management. Owing to great variability in the ores available, Chinese iron works produce iron of varying composition, as shown in Table 1.

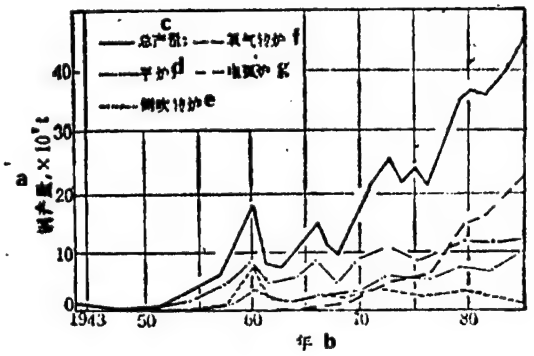

Fig. 1. China's steel output

Key:
a. Steel output, million tons
b. Year
c. Total output
d. Open hearth furnaces
e. Side-blown converters
f. Oxygen-blown converters
g. Electric arc furnaces

Table 1. Composition of steelmaking iron produced by certain enterprises, percent

a 元 素	C	Si	Mn	S	P	b 其 它
c 鞍 钢	4.48	0.66	0.17	0.024	0.071	
d 首 钢		0.35	0.40	0.023	0.040	
e 武 钢		0.86	0.16	0.021	0.096	Cu<0.1 (60年代为0.3)m
f 包 钢	4.88	0.68	1.42	0.035	0.444	Nb 0.04 (60年代为0.08)n
g 攀 钢		0.10		0.058	0.043	V 0.31, Ti 0.145
h 本 钢		0.78	0.39	0.036	0.043	V 0.28, Ti 0.17
i 马 钢		0.55	0.12	0.034	0.318	As 0.039～0.051
j 柳 钢		0.90	0.30	0.045	0.350	Cu 0.169, As 0.035
k 涟 钢		0.68	0.25	0.027	0.494	
l 日本（参考）		0.3～0.4	0.55	0.030	0.100	

Key:
a. Element
b. Other
c. Anshan
d. Capital
e. Wuhan
f. Baotou
g. Panzhihua
h. Benxi
i. Ma'anshan
j. Liugang
k. Dalian
l. Japan (for comparison)
m. (0.3 in the 1960's)
n. (0.08 in the 1960's)

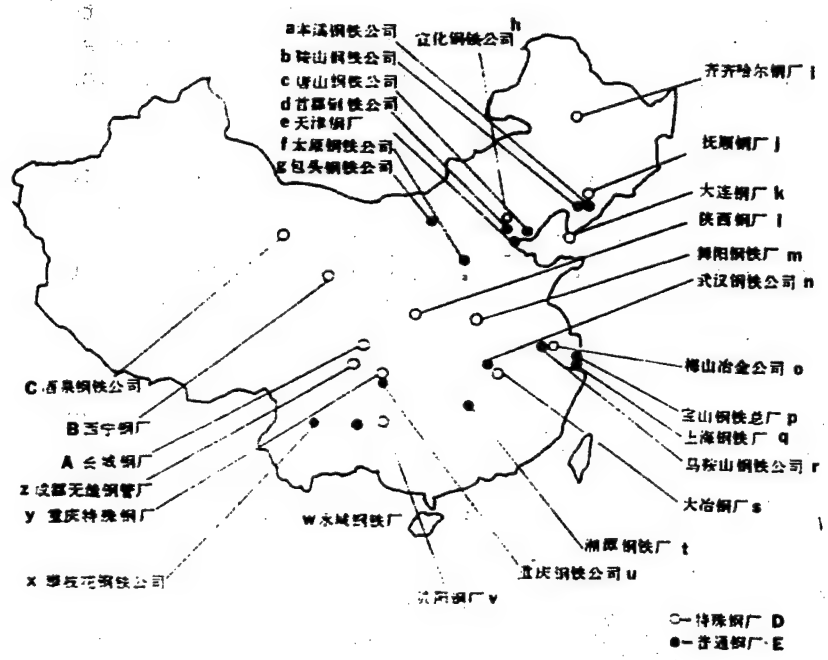

Fig. 2. Locations of principal iron and steel enterprises

Key:

a. Benxi Iron and Steel Complex
b. Anshan Iron and Steel Complex
c. Tangshan Iron and Steel Complex
d. Capital Iron and Steel Complex
e. Tianjin Steel Works
f. Taiyuan Iron and Steel Complex
g. Baotou Iron and Steel Complex
h. Xuanhua Iron and Steel Complex
i. Qiqihar Steel Works
j. Fushun Steel Works
k. Dalian Steel Works
l. Shaanxi Steel Works
m. Wuyang Iron and Steel Works
n. Wuhan Iron and Steel Complex
o. Meishan Metallurgical Complex
p. Baoshan Iron and Steel Complex
q. Shanghai Iron and Steel Works
r. Ma'anshan Iron and Steel Complex
s. Daye Steel Works
t. Xiangtan Iron and Steel Works
u. Chongqing Iron and Steel Complex
v. Guiyang Steel Works
w. Shuicheng Iron and Steel Works
x. Panzhihua Iron and Steel Complex
y. Chongqing Specialty Steel Works
z. Chengdu Seamless Steel Pipe Works
A. Changcheng Steel Works
B. Xining Steel Works
C. Jiuqan Iron and Steel Complex
D. Specialty steel works
E. Ordinary steel works

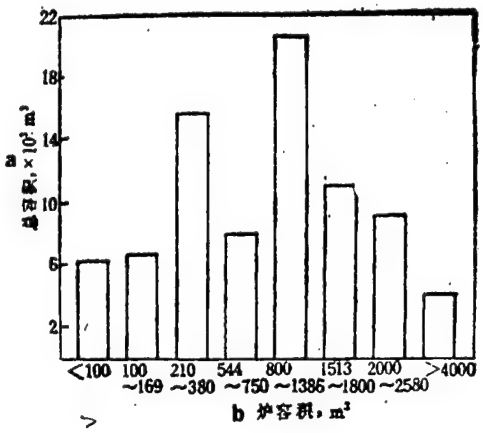

Fig. 3. Distribution of capacity by blast furnace size

Key:
a. Total capacity, thousand m^3
b. Furnace capacity, m^3

China's technical development has been a combination of continuity and innovation. Some important progress was made during the Great Leap Forward and the Cultural Revolution despite the disruptions of these periods. Faced with a shortage of chromium-containing materials for refractory brick, China developed a magnesia-alumina brick for open-hearth furnaces. The Panzhihua technique for dealing with high-tatanium ores, mentioned above, is another example. It also developed an atomization technique for recovering vanadium from molten iron. A process for recovering nickel and manganese from blast furnace slag was developed at the Baotou complex before the Cultural Revolution.

Progress in blast furnace practice in the period from 1976 to 1985 is indicated in Fig. 5, which shows an increase in the effective volume utilization factor and a decrease in the coke ratio and the fuel ratio with increasing furnace temperatures. Coal powder has partially or wholly replaced oil as an injection material in blast furnaces. Other advances include high-pressure furnace bells (used in blast furnaces that account for more than 60 percent of capacity), high-alkalinity ore agglomeration, and the use of techniques to decrease the silica content of molten iron. Reconstruction of the Capital Iron and Steel Complex No 2 blast furnace in 1982 added numerous modern features: pre-screening of ore, use of belt containers, a non-charging bell, use of a top pressure of 15 newtons per square centimeter, a top-burning blast stove and the like. The utilization factor of this blast furnace rapidly rose to about 2.0.

Combined-blow converter practice has expanded rapidly. By 1985 it was in use in 32 top-blown converters in 19 converter shops, where it increased output, decreased materials loss and increased furnace life. The use of oxygen in open hearth furnaces (primarily top-blown) greatly increased capacity and decreased energy consumption. The Anshan, Wuhan and Baotou Iron and Steel Complexes also decreased the number of open-hearth furnaces they had in operation. Effective features introduced from abroad include sliding taps, slag-skimming steel tapping, nitrogen injection into ladles, the use of insulating slabs to protect castings. Many steel mills have introduced powdered coal treatment, "wire feed" treatment, vacuum treatment, nitrogen-oxygen treatment and other out-of-furnace techniques.

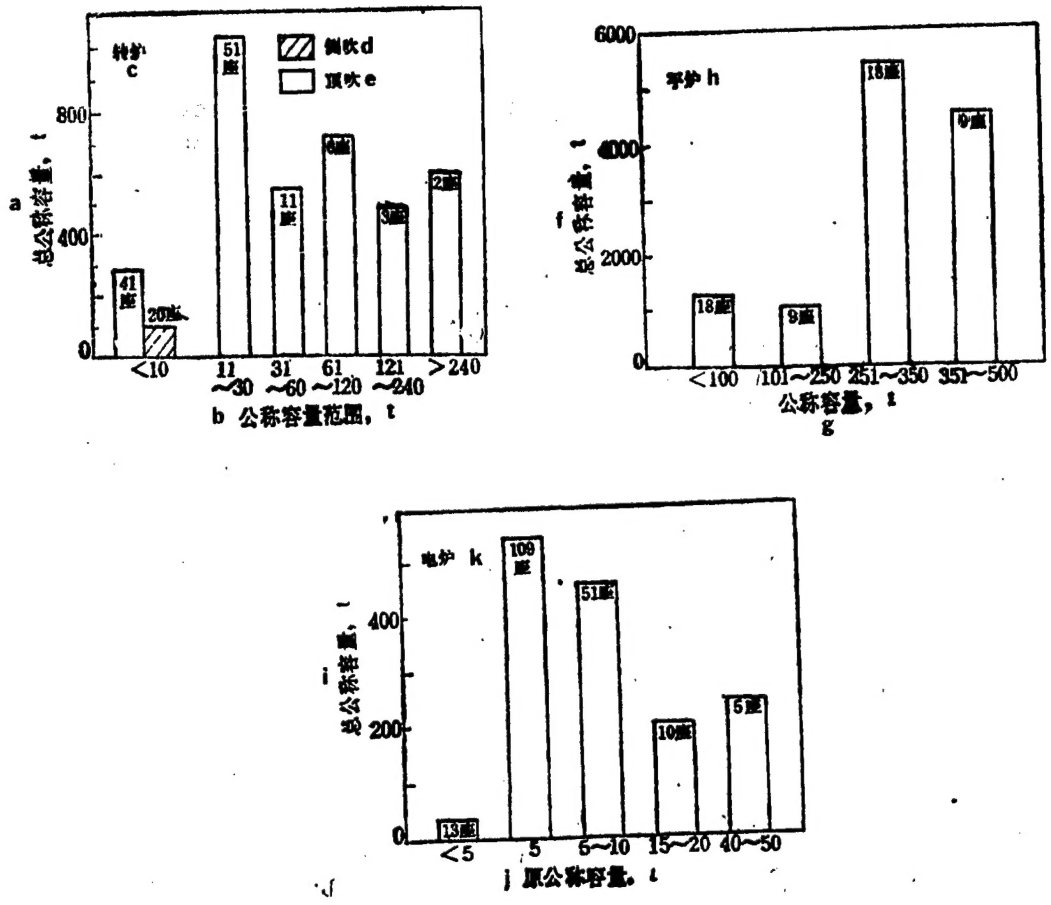

Fig. 4. Distribution of capacity among converters, open hearth furnaces and electric furnaces of various sizes

Key:
a. Total nominal capacity, tons
b. Nominal capacity range, tons
c. Converters
d. Side-blown
e. Top-blown
f. Total nominal capacity, tons
g. Nominal capacity, tons
h. Electric furnaces
i. Total nominal capacity, tons
j. Original nominal capacity, tons
k. Electric furnaces

There has been considerable progress in low-alloy and alloy steels. The national output of high-strength low-alloy steel had reached 13.2 percent of total steel output in 1985. While manganese and manganese-silicon steels were formerly the principal types, currently nickel, vanadium and titanium steels using Chinese ores are being developed.

The expansion of continuous casting is particularly noteworthy (see Fig. 6); it accounted for 10.75 percent of all steel casting in 1986. At least half of the output is continuous-cast at seven shops or steelworks, including the Wuhan complex's No 2 plant, which in 1985 became the first facility to use exclusively continuous casting.

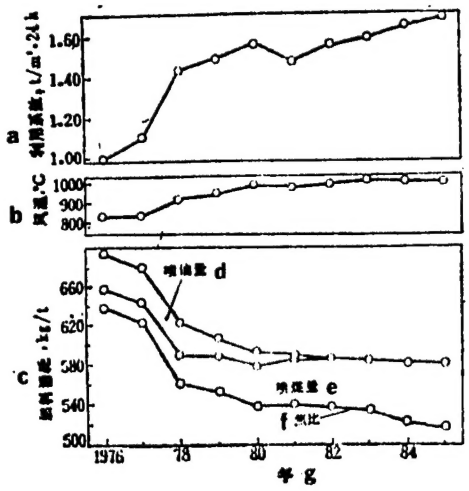

Fig. 5. Average blast furnace utilization factor, temperature and fuel consumption at key enterprises

Key:
a. Utilization factor, tons per cubic meter per 24 hours
b. Blast temperature, degrees C
c. Fuel consumption, kg/ton
d. Oil injection
e. Coal injection
f. Coke ratio
g. Year

Waste gas recovery has now been introduced in nine converter shops.

An important step in refractory technology is the development of two-step calcination of basic refractory materials.

In the next 10 years, in addition to large-scale conventional blast-furnace-based iron and steel works and electric furnace facilities, it will be necessary to develop relatively small, high-efficiency plants of other types. In addition it will be necessary to renovate and modernize medium and small-size plants operating on the blast furnace-converter cycle to increase their efficiency and decrease costs. The use of non-blast-furnace technologies is of great economic importance in these respects.

An examination of the energy costs of several foreign direct reduction or melt reduction techniques (the KR, plasma fusion and Midrex processes) is inconclusive, since it indicates that local materials availability and cost strongly influence the economic results. Whether direct reduction and melt reduction should be included among the non-blast-furnace techniques to be used will require careful study because plants using these techniques are often highly specialized.

Another set of approaches whose feasibility is highly dependent on specific conditions is pretreatment of molten iron to change the levels of various impurities. Impurity levels can also be affected by the choice of materials in the blast-furnace charge, by the steel refining procedure itself, and by post-treatment of the molten steel. The sulfur content of molten iron can be decreased by shallow desulfuring of large heats or deep desulfuring of small heats, as is the practice in the No 2 plant at the Wuhan Iron and Steel Complex and by the Baoshan complex. Injection of powdered materials into the ladle to remove sulfur is also possible. Progress in sulfur removal technology may make pretreatment of molten iron to remove sulfur an attractive approach. Removal of silicon is more complicated. Silicon is both a slag-forming element and a heat-producing element in steelmaking, and too low a silica content may hinder converter operation, as at the Panzhihua complex.

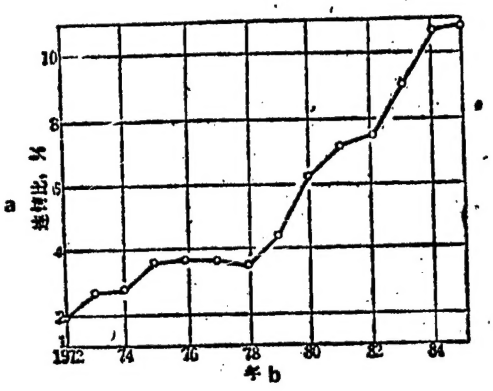

Fig. 6. Percentage continuous casting

Key:
a. Continuous casting, percent
b. Year

In addition, a high silica content in pig iron is useful when increasing the amount of steel scrap used in the converter charge. Since China's mine and blast furnace capacity are insufficient to support its steel-making capacity, it increases its output by adding large amounts of steel scrap (some of it purchased abroad) to converter charges; thus removal of silica from molten steel is not currently attractive.

As regards phosphorus removal, the Anshan, Benxi, Wuhan and Capital Iron and Steel Complexes produce low-phosphorus molten iron in any case; in addition, since China uses large amounts of scrap steel in steelmaking and has a low demand for low-phosphorus steel, there is little reason to pursue phosphorus-removal pretreatment.

The development of the bottom-blown oxygen converter in the 1960's made combined-blowing technology possible. China chiefly used bottom-blown nitrogen stirring of the melt pool. Some plants switched over partially or wholly to argon. It was later found abroad that bottom blowing with oxygen mixed with powdered lime produced better refining results. Various versions of this approach were adopted by Chinese plants.

In the new West German Klockner process, oxygen and coal dust are blown into the converter to provide an external heat source, thus allowing the amount of steel scrap in the charge to be increased. Such a technique would solve various problems of China's steel industry: (1) the powdered coal could replace diesel fuel as a lance cooling material; (2) it would provide sufficient heat when 50 percent scrap is used in the converter; (3) it would replace superior grade metallurgical coke when refining cupola furnace iron; (4) it would allow the steel scrap ratio in the converter to be increased, thus making increased steel output less dependent on blast furnace construction. With the approval of the Ministry of Metallurgy, this process was upgraded from laboratory trials to pilot commercial production in 1982 and gave satisfactory results in three campaigns on a converter with a capacity of 8 tons. It will be extended to larger converters in order to increase the proportion of scrap used in them.

This technique is also usable as an end reduction method in melt reduction. The Krupp works has put in a great deal of effort on this process. It apparently could be coupled with shaft-furnace pre-reduction (as is done by Krupp) or with fluidized-bed pre-reduction. Melt reduction appears to be a promising topic for research.

8480/7358
CSO: 4008/0074

END